Diffusion-limited recombination in polymer-fullerene blends and its influence on photocurrent collection

Jenny Nelson
Centre for Electronic Materials and Devices, Department of Physics, Imperial College of Science, Technology and Medicine, London SW7 2BW, United Kingdom

(Received 19 September 2002; revised manuscript received 3 December 2002; published 30 April 2003)

We propose a model of charge recombination in interpenetrating two-phase systems, and apply it to blends of poly [2-methoxy-5-(3′,7′-dimethyloctyloxy)-1-4-phenylene vinylene], (MDMO-PPV) and 1-(3-methoxycarbonyl)-propyl-1-phenyl-(6,6)C_{61} (PCBM). The main features of the model are that charge recombination is rate limited by the diffusion of positive polarons towards PCBM anions; that the density of polaron states contains a tail of deep traps which serve to delay recombination; and that polarons move between localized states largely by means of thermally activated hopping. The model is implemented using Monte Carlo simulations and is applied to reproduce the observed dependence of charge recombination kinetics on laser intensity, temperature, and background illumination, detected by transient optical spectroscopy. Modeling the experimental data yields a density of deep localized states in MDMO-PPV of order 10^{17} cm^{-3}, and a charge carrier lifetime of order 10 μs under solar illumination. An alternative model based on direct tunneling is ruled out by comparison with the observed temperature dependence. The recombination model is incorporated into a one-dimensional calculation of short-circuit photocurrent in a solar cell as a function of temperature and light intensity. We conclude that charge recombination is sufficiently slow not to limit photocurrent collection under solar intensities at short circuit, and propose that space charge effects may be responsible for the observed sensitivity of photocurrent to temperature.

DOI: 10.1103/PhysRevB.67.155209 PACS number(s): 73.23.−b, 73.61.Ph, 78.66.Qn

I. INTRODUCTION

Interpenetrating networks of electron transporting and hole transporting materials are of growing interest and importance for photonic and electronic applications. Phase separation on the nanometre scale creates a large surface area for dissociation of photogenerated charge pairs, while continuous pathways in each material allow for charge conduction to external electrodes. Such interpenetrating systems have been used to enhance photocurrent generation in semiconducting polymers[1–4] and in dye-sensitized metal oxide[5] and semiconducting[6] electrodes permeated with electrolyte, and to enhance the response of photodiodes[7] field effect transistors,[8] and other devices.

Blends of hole transporting conjugated polymer and electron accepting fullerene derivatives are particularly promising materials system for thin film, organic solar cells.[9] Devices with power conversion efficiency over 3% have been demonstrated.[10,11] The efficient function appears to be due to the combined effects of ultrafast electron transfer from photoexcited polymer to fullerene,[12] a large interfacial area for charge separation due to intimate blending of the materials,[11] and efficient carrier transport across the thin film.

Kinetics of charge recombination are critical to device performance relevance. High recombination losses may be expected on account of the large interfacial area, yet these are evidently low enough to allow efficient charge carrier collection across thin films, resulting in external quantum efficiencies of over 50%.[11] Recent studies of charge recombination in poly(2-methoxy-5-(3′,7′-dimethyloctyloxy)-1-4-phenylene vinylene/1-(3-methoxycarbonyl)-propyl-1-phenyl-(6,6)C_{61} (MDMO-PPV/PCBM) blends[13,14] using transient optical spectroscopy have revealed a number of interesting features, notably that two phases are present in the kinetics following laser pulse excitation, a fast phase whose amplitude is strongly intensity dependent, and a slow phase whose amplitude saturates with increasing laser intensity. The slow phase decays as a power law with time and is thermally activated. The kinetics accelerate in the presence of background light, but are insensitive to fullerene concentration except on the slowest (~ms) time scales.

The presence of the two distinct phases and the saturation of the slow phase with light intensity cannot be explained with simple models of diffusion limited or Coulomb-interaction driven recombination. Those models would lead to a monophasic decay with light-intensity dependent amplitude on all time scales. However, the results are qualitatively compatible with a model where charge recombination is limited by the diffusion of positive polarons towards electrons located on PCBM anions, and polaron diffusion is mediated by trapping and release from a limited number of deep traps. This is in contrast to previous studies which invoked direct tunneling as the mechanism for charge recombination in such systems at low temperature.[15] In this paper we present the details of the multiple trapping model, and demonstrate that tunneling transport cannot explain the experimental observations unless thermally assisted. We implement the model using Monte Carlo simulations to reproduce experimental results, derive values of the parameters relevant to device function, and apply the findings to the problem of photocurrent generation in a plastic solar cell.

The paper is set out as follows. In Sec. II the models are described and qualitative results presented; in Sec. III experimental data from Refs. 13 and 14 are modeled and param-

eters extracted; results are discussed in Sec. IV; and in Sec. V a model for photocurrent generation in a device is presented.

II. MODELS

The model is required to simulate charge carrier density as a function of time after photogeneration by a laser pulse. Charge carriers are generated as pairs by a laser pulse at time $t=0$, at a density p_0 where p_0 is the density of absorbed photons multiplied by the charge separation efficiency. As time proceeds the charge carrier density is reduced by charge recombination events. Note that the experiments in Refs. 13 and 14 are effectively carried out at open circuit. There is no current collection to compete with charge recombination. We consider two mechanisms for charge carrier recombination, diffusional encounters via a thermally activated random walk, which we call ''multiple trapping,'' and direct recombination via a series of polaron tunnelling events, called ''multistep tunneling.'' Such models were first developed to model charge transport in amorphous inorganic materials[16,17] and variants have been applied to polaron transport in organic electronic materials.[18–20] More recently, similar models have been adapted to simulate electron transfer in dye sensitized electrodes.[21,22] In both the multiple-trapping and tunneling cases we consider the positive polaron on the polymer to be the mobile species and the negative charge on the fullerene anion to be fixed. This is justified below.

The transport landscape for the polaron is modeled as a lattice of discrete sites, of energy drawn from a density of states function $g(E)$. Each site represents, approximately, one hole transporting unit (one monomer) of the polymer and the intersite distance is chosen to correspond to the mean intermonomer distance if the polymer were arranged as a cubic lattice of monomers. The different energies represent both energetic disorder due to conformational variation, and deep traps due to chemical defects. For the modeling in this paper we use a bimodal density of states containing a fraction $(1-\phi)$ of ''transport'' states, with energy close to the highest occupied molecular orbitals (HOMO) level, E_0, and a fraction ϕ of localized sites whose energies are drawn from a density of localized states, $g_1(E)$. The delocalized fraction may be considered as lying above a mobility edge.

Each lattice site may be occupied, vacant or contain a fullerene anion. Strictly, the lattice represents a random blend of polymer and fullerene molecules in a ratio such that continuous pathways exist for charge conduction within each material. For photocurrent generation it is critical that such pathways exist. However, in transient optical experiments where no electrodes are present and there is no current flow, the existence or otherwise of continuous pathways is not relevant. Additional modeling, summarized in Sec. IV, of charge recombination has shown that the relevant parameter is the density of fullerene *anions* and not the overall fullerene density. This is consistent with observation. Therefore, for simplicity, we incorporate only fullerene anions into the model and do not distinguish between sites which do and do not contain a neutral fullerene molecule. Periodic boundary conditions are applied in all three dimensions. This is valid in the case of low optical density where excitons are generated uniformly across the film. Interfacial effects are not included.

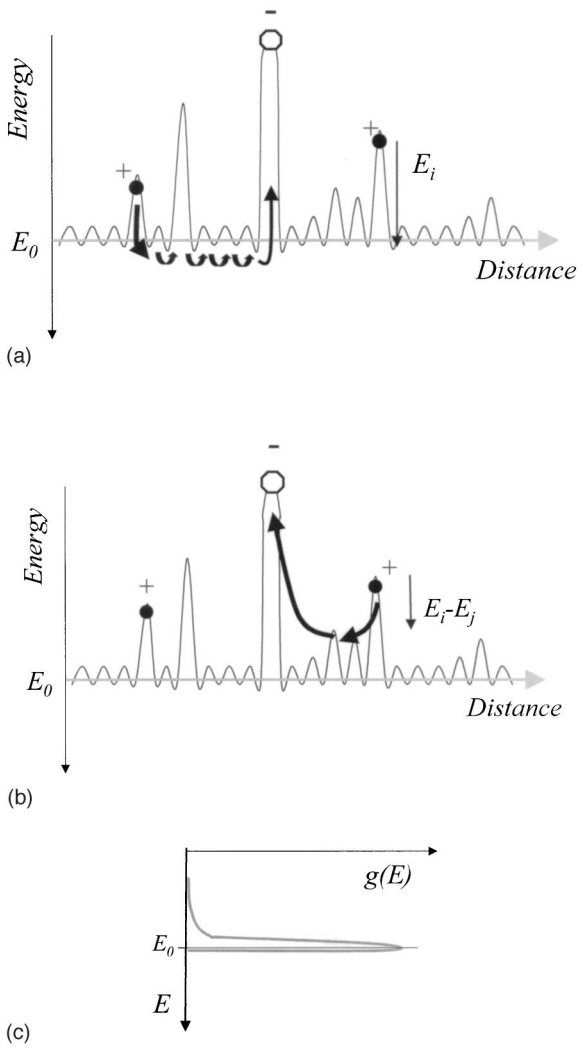

FIG. 1. Schematic of charge recombination in the cases of (a) thermal activation to HOMO level E_0 and (b) thermally assisted multistep tunneling. The fullerene anion (octagon) is represented as a deep potential well for the polaron. In (a), the polaron is activated through energy E_i to the HOMO level, and reaches the fullerene by a sequence of nearest neighbor steps. In (b) the polaron reaches the fullerene by a sequence of tunnelling events. (c) shows a bimodal density of states function, consisting of a narrow Gaussian centred around the HOMO level and a long exponential tail. Note that increasing polaron energy is measured *down* from the HOMO level.

Transport is simulated using either the multiple trapping or the multi-step tunneling model. The multiple trapping model is illustrated in Fig. 1(a). In this picture, polarons move by thermal activation over a barrier set at the HOMO level into one of the available neighboring sites. The time for release from a site of energy E is given by

$$\tau = -\ln X \frac{1}{\nu_0} \exp\left(\frac{E_0 - E}{kT}\right), \tag{1}$$

where E_0 is the energy of the HOMO level, ν_0 the attempt-to-jump frequency, X a random number between 0 and 1, k is Boltzmann's constant, and T the temperature. Note that we adopt the convention where increasing hole energy is measured *down* from the HOMO level, E_0 [see Fig. 1(c)]. The destination site is chosen at random from the nearest neighbors available. When the polaron arrives on a site occupied by a negative charged fullerene, both charges are removed.

In the multistep tunneling model, illustrated in Fig. 1(b), polarons move by tunnelling to other available sites in the polymer, with the hopping time from initial site i to final site j given by

$$\tau = -\frac{\ln X}{\nu_{pp}} \exp\left(\frac{2R_{ij}}{a_0}\right) \exp\left(\frac{\Delta E_{ij}}{kT}\right), \tag{2}$$

where

$$\Delta E_{ij} = \begin{cases} E_j - E_i & \text{if } E_j > E_i \\ 0 & \text{if } E_j \leqslant E_i, \end{cases} \tag{3}$$

and R_{ij} is the spatial separation of sites i and j, a_0 is the Bohr radius or ''localization radius'' for the positive polaron, and ν_{pp} the attempt to jump frequency for hole tunneling between polymers. Note that although the localization radius is formally expected to depend on the hole affinity of the initial site, the variation in a_0 over the range of energies considered here is sufficiently small that a_0 may be considered constant. Using energy dependent a_0 makes no significant difference to the results.

The Miller-Abrahams energy dependent factor in the hopping time [Eq. (2)] allows thermally assisted tunneling. Polarons may also tunnel directly to sites occupied by a negatively charged fullerene, in which case the charges recombine. The hopping time to a fullerene anion at site j is given by

$$\tau = -\frac{\ln X}{\nu_{pn}} \exp\left(\frac{2R_{ij}}{a_0}\right). \tag{4}$$

The rate ν_{pn} may differ from ν_{pp} on account of different rates for hole tunneling from polymer to a fullerene anion and to a neutral polymer site due, for instance, to the different electronic orbitals. Although the hopping time for this process may also depend upon the polaron site energy, the variation in polaron energy is expected to be small compared to the driving force for this reaction, and so we have assumed τ to be energy independent.

Every time a polaron arrives at a new site, waiting times for all possible steps are generated from Eqs. (2) and (4). The shortest time is identified, and the corresponding destination is selected. In this model, the relative importance of tunneling relative to thermal activation is determined by the localization radius, and by the ratio ν_{pn}/ν_{pp}, which reduces the number of tunneling events required for recombination.

In both models the sequence of polaron motions is determined by assigning waiting times to the carriers in the system and sorting them into a queue. All polarons in the ensemble possess a waiting time and a destination. At each step in the iteration, the polaron with the shortest waiting time, t_1, moves to its destination, the simulation time is advanced by t_1 and the waiting time of all remaining carriers is reduced by t_1. If the polaron arrives at a site occupied by a fullerene anion, it is removed from the queue and the anion is deleted. If not, a new waiting time and destination are assigned and it is re-entered into the queue. The procedure is repeated for the polaron now at the top of the queue. The device of the queue enables several moving particles to be handled at once, and trap filling effects are included through a rule preventing multiple occupancy of sites ensuring consistency with Fermi-Dirac statistics.[21,23] In these respects the model differs from the classical continuous time random walk.[16]

In the case of laser pulse photogeneration under background light, ''background'' charge carrier pairs are generated at a given average rate and allowed to diffuse and recombine as usual. The laser pulse adds an additional density, p_0, of charge pairs at $t=0$. No distinction is made between background light generated and laser pulse generated charges nor between charges generated by different wavelengths of light. To simulate different background light intensities, we first find the steady state carrier density, p_{ss}, under a given generation rate without laser pulse. We then start simulations with an average carrier density of p_{ss} present before the laser pulse, and record the *net* number of recombination events (recombination less generation events) following the laser pulse. The steady state simulations also yield the dependence of steady state carrier density on light intensity for any given density of states function and recombination parameters.

The following physical assumptions are implicit in the model: (i) Photogeneration is uniform. This is justified by the low optical density of the sample, of 0.5, at the pump wavelength. (ii) The quantum efficiency for exciton dissociation is unity. This follows from previous reports of fast and efficient charge separation in blends containing over 5% by weight of fullerenes.[12] (iii) The recombination is non-geminate, i.e., the charges resulting from exciton dissociation are generated with sufficient kinetic energy to escape each other, as argued from experimental data in Ref. 13. Geminate recombination might be expected for a low pump photon energy, where the exciton is generated in a segment of small optical gap and is less likely to dissociate by downward hopping or diffusion, or at low temperatures, but neither is relevant for the data modeled here; (iv) negative charges on fullerene anions are immobile. This follows from the observation in Ref. 14 that the fullerene concentration has negligible effect on the recombination kinetics, except on the longest (~ms) time scales. It is stated below that relaxing this assumption has no significant effect. (v) Coulomb interactions are neglected. The final assumption is addressed in Sec. IV below.

The following parameters are required for the modeling of transient optical data: lattice constant a, fraction of localized sites ϕ, energy distribution of localized states $g_1(E)$, attempt to jump frequency ν_0, temperature T, polaron generation density p_0 at each laser pulse intensity, the extinction coefficient of the polaron at the probe wavelength ε_{ext}, and,

in the case of background light, polaron generation rate for the appropriate background light intensity. In the case of thermally assisted hopping, the localization radius a_0 and the rates ν_{pp}, and ν_{pn} are also needed. In the case of multiple trapping, there is an additional implicit parameter: the cross section for recombination of polaron with a fullerene anion. In our model this is effectively the area of a lattice cell, a^2, since the arrival of a polaron at a negative charge site invariably results in recombination. Changing this recombination cross section cannot be distinguished from changing the attempt to jump frequency, except in the (inappropriate) limit of very small recombination cross section where the rate determining factor is achieving a sufficiently high number of diffusional encounters of the charge pair, and activation out of localized states becomes irrelevant.

Before addressing the experimental data, we first present some preliminary results to illustrate the effect of the density of states and choice of model on the shape of kinetics. The experimental data[13,14] follow a power law,

$$p \propto t^{-\alpha}, \tag{5}$$

of exponent $\alpha \sim 0.4$, over four orders of magnitude in time, assuming that the change in absorbance is proportional to p. Such power law kinetics are known to follow for a process which is limited by thermal emission from an exponential density of trap states of the form

$$g_l(E) = \frac{N}{kT_0} \exp\left(\frac{E - E_0}{kT_0}\right), \tag{6}$$

where N is the total density of localized states,

$$\alpha = T/T_0 \tag{7}$$

and $T > T_0$. [The form of Eq. (5) is easily verified by summing contributions of the form $e^{-t/\tau}$, with $\tau(E)$ given by Eq. (1), with respect to energy over a distribution of type Eq. (6).] As expected, simulations with the multiple trapping model produce this behavior for an exponential density of states with all states localized ($\phi = 1$), i.e., thermal activation out of traps dominates the recombination kinetics. If the exponential $g_l(E)$ is replaced by a Gaussian tail of the form

$$g_l(E) = \frac{N}{\sqrt{2\pi}\sigma} \exp\left(-\frac{(E - E_0)^2}{2\sigma^2}\right);$$

then an approximate power law behavior can be obtained with slope $\alpha \sim 0.4$ using a half width σ of 6–10 kT, but only over 2–3 orders of magnitude in time, so a single Gaussian tail could not explain the experimental data. In the following we adopt an exponential $g_l(E)$ as the simplest form which produces a power law in $p(t)$. However, other forms are known which can also produce power law behavior over several orders in time, such as the sum of two Gaussians, possibly representing two distinct trap levels of different energy and incidence.[23]

Figure 2 illustrates the dependence of polaron density on laser pulse intensity for two limiting models, the multiple trapping [Fig. 2(a)] and multi-step tunneling with a long localization radius, $a_0 = 4a$ [Fig. 2(b)]. In both cases the density of states contains a fraction $\phi = 0.01$ of trap states drawn from an exponential distribution with $\alpha = 0.4$; the remainder are isoenergetic. The family of curves in Fig. 2(a) show the characteristic power law behavior at long times, $p \propto t^{-\alpha}$, expected from Eqs. (1), (6), and (7) above. At short times the behavior depends on p_0. For sufficiently high values of p_0, a separate phase with faster kinetics can be resolved, which is due to the saturation of the available trap states. In that limit the first recombination events are limited by the availability of anions, not by thermal activation out of traps, and follow bimolecular kinetics until the *untrapped* polarons are all gone. After this, the thermal activation of the *trapped* polarons becomes limiting and the power law decay appears. This change in behavior gives rise to a point of inflection in the kinetics on the log-log scale. Such a feature is character-

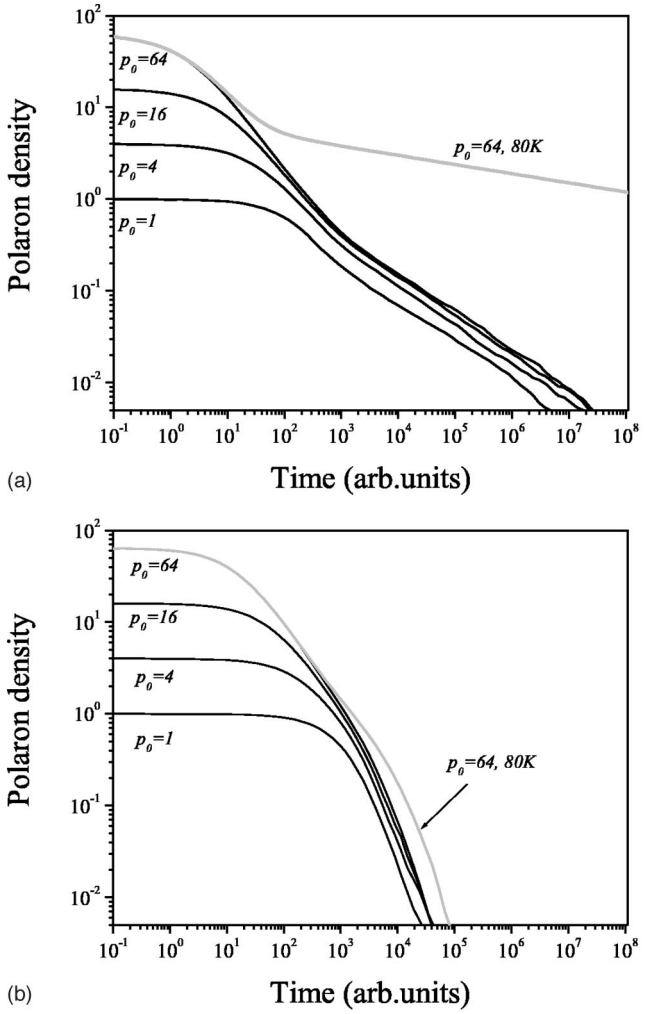

FIG. 2. Simulated polaron density as a function of time after photoexcitation for different laser pulse intensities for the cases of (a) thermal activation and (b) multistep tunneling with $a_0 = 4a$. *F*. In both cases, black curves represent 1, 4, 16 and 64 photogenerated charge pairs at 300 K in a simulation volume of 10^3 sites containing 1% traps from a distribution with $T_0 = 750$ K. The gray curve represents 64 photogenerated charge pairs at 80 K. Notice that the multi-step tunneling model is almost temperature independent for this large value of a_0. For values of $a_0/a \leqslant 1$, the tunneling model reproduces the behavior shown in (a), at all temperatures studied.

istic of the experimental data. In this model, the slope of the power law, α, depends directly upon temperature as $\alpha = T/T_0$, as illustrated for two different temperatures in Fig. 2(a). As discussed below, this temperature dependence is also a feature of the data. The behavior as $t \to \infty$ is determined by the low energy cut off of $g_l(E)$. For instance, a flat cutoff produces an exponential tail in p at long times.

The different behavior for carriers above and below a certain threshold energy level is consistent with the notion of a mobility edge. Carriers at energies within kT of the HOMO level are readily activated and may be considered ''free,'' while carriers in deeper energy states are localized. In the multiple trapping model, both charge transport and recombination are due to the free carriers. For a simple exponential density of states function the fraction above a certain energy threshold is related to the total polaron density by

$$p_{\text{free}} = Ap^{\beta}, \tag{8}$$

where $\beta = 1/\alpha$ for a pure exponential,[23] though the exponent may be different for a bimodal density of states.

Figure 2(b) shows a family of curves for the multiple step tunneling model. We illustrate the case where a_0 is large compared to the lattice constant ($a_0 \gg a$) and $\nu_{pn}/\nu_{pp} = 1$. A clear power law behavior is not produced and the point of inflection is absent; this is the case for all values of ν_{pn}/ν_{pp} and ϕ studied. For such large a_0 the kinetics are insensitive to the form of the density of states and to temperature. In contrast, in the limit where $a_0 < a$, the kinetics are dominated by thermal activation and the results of the multiple trapping case are reproduced. In that limit the value of ν_{pn}/ν_{pp} affects only the overall time scale of the kinetics, and the slope α depends upon density of states and temperature exactly as for case of Fig. 2(a).

From this we conclude that in order to reproduce the observed temperature dependent power law behavior we need to use a thermally activated model. Although multistep tunneling may be a more appropriate general description of charge transport in polymers, in the limit where the spacing between traps states is more than several localization radii, polaron motion is effectively by nearest neighbor hopping and the multiple trapping model is an excellent approximation.

III. RESULTS

In this section we present the results of modeling the transient absorption data in Refs. 13 and 14. The data were taken on 100 nm thick films of MDMO-PPV on glass, containing PCBM in a ratio of 1:2 or 1:4 MDMO-PPV:PCBM by weight. The films were pumped at 500 nm with laser pulses of power between 20 nJ and 80 μJ over a 1-cm^2 area, and probed at 960 nm where the PPV polaron is found to absorb.[13] The optical density of the film at 500 nm is sufficiently low (0.5) that uniform photogeneration is a reasonable approximation.

The system was simulated using a lattice of size $40 \times 40 \times 40$ with periodic boundary conditions. This represents a volume of 2.7×10^{-17} cm^3, taking the lattice constant a as 0.75 nm (from molecular weight and density of MDMO-PPV). A laser power of 1 μJ cm^{-2} corresponds to absorption of 1.5×10^{17} photons per cm^3, corresponding to four photogeneration events in the simulation volume. For unit dissociation efficiency, 1 μJ generates four polarons and fullerene anions in the simulation volume. The polaron extinction coefficient at the detection wavelength of 960 nm, ε_{ext} was taken as 60 000 dm^3 mol^{-1} cm^{-1}, from the observed change in absorbance due to a 1-μJ laser pulse assuming no losses to recombination at times shorter than 100 ns for that laser power.

The remaining parameters were chosen as follows: the T_0 of the density of localized states was chosen as 750 K, to produce the observed value of 0.4 ± 0.05 at 300 K. The fraction of localized states was chosen as 0.001 to produce the emergence of the fast phase at the correct laser power. This represents a density of localized states of 2.4×10^{18} cm^{-3}, of which only a fraction are deep enough to function as traps, e.g., around 3×10^{17} cm^{-3} sites are more than 5 kT below the HOMO level. The transport states are assumed isoenergetic at E_0, but similar results are obtained for a Gaussian distribution of transport states with half width $\leqslant 50$ meV. The attempt to jump frequency was then chosen as 1.25×10^{11} s^{-1} to fit the absolute time scales. Modeling was done using the multiple trapping model. This was justified by the observation, mentioned above, that the tunneling model with $a_0 < 2a$ produces virtually identical results. Although the extent of the localized polaron wave function in MDMO-PPV is not known, it has been estimated as around 1 nm.[15] This is likely to be an upper limit, as localization radii in molecular materials are usually sub-nm[24] on account of weak van der Waals interactions.

Figure 3 shows the simulated optical density transients for four different laser pulse powers, in comparison with data from Ref. 14. The change in absorbance, ΔA, is obtained from

$$\Delta A = \frac{1000 p \varepsilon_{\text{ext}} d}{N_A},$$

where N_A is Avogadro's number, d is the sample thickness in cm (10^{-7} cm) and p is in units of cm^{-3}. The model reproduces the main features of the data: a fast, laser power dependent phase, due to prompt recombination by ''free'' polarons; the saturation of signal with light intensity at long times, due to recombination being limited by emission from a limited number of traps; and sensitivity of the slow phase to laser power at pulse energies less than 1 μJ. Using the multiple trapping model in place of the thermally activated model produces identical results, to within a small time scale factor, for $a_0 < 2a$.

In Fig. 4 we present the modeled behavior at two different temperatures, 220 and 300 K, and a laser power above threshold (8 μJ/pulse). All other parameters are the same as for Fig. 3. As the temperature is reduced to 220 K the exponent of the simulated transient reduces to 0.3, as expected from Eqs. (5) and (7), in good agreement with the data. However, the model predicts a higher amplitude than observed for the lower temperature decay. As the temperature is reduced further, the multiple trapping model predicts a con-

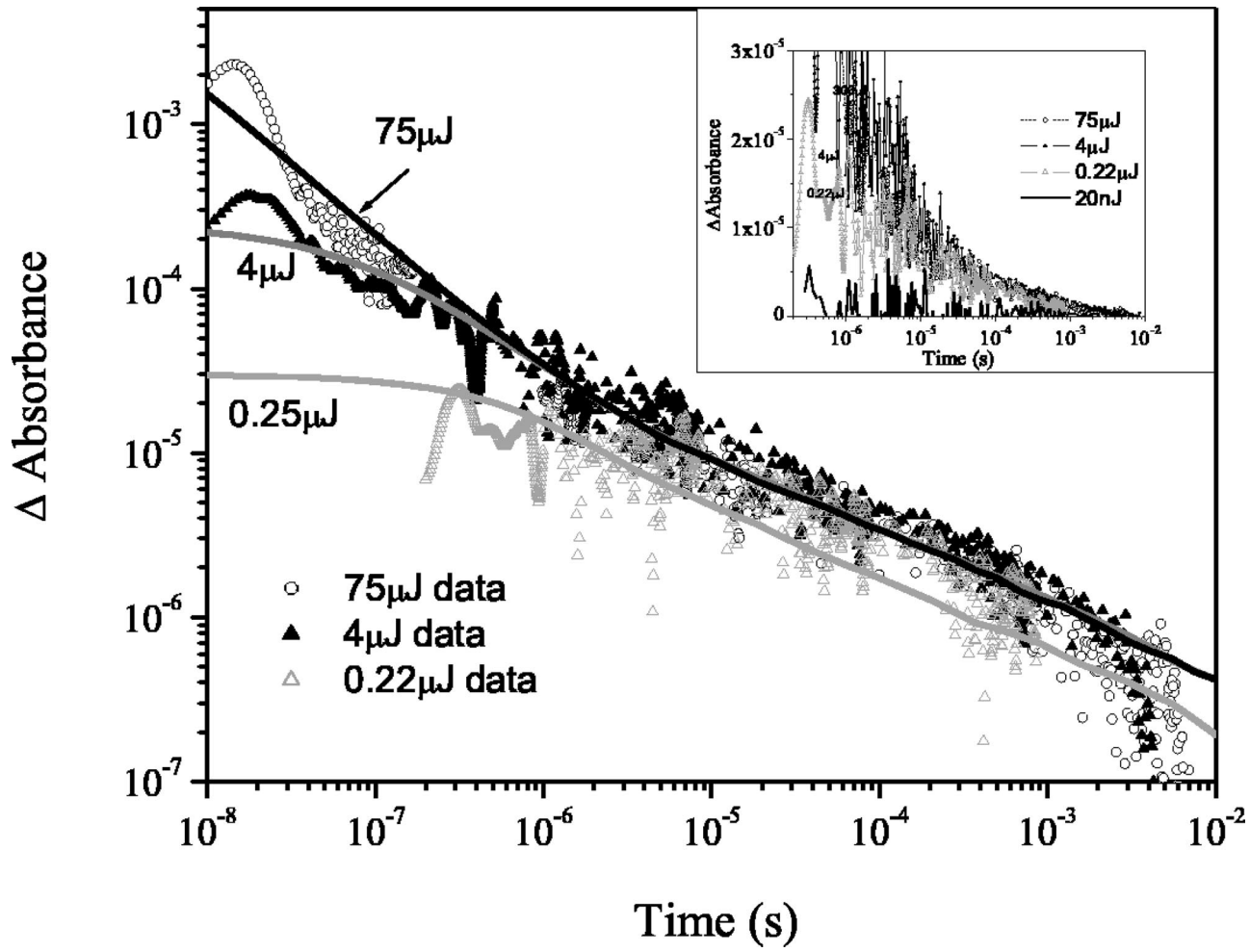

FIG. 3. Measured and modeled recombination kinetics at 300 K at laser intensities of 0.22, 4, and 75 μJ per pulse. Modeling was done using the multiple trapping model with 0.1% of sites drawn from an exponential density of localized states with $T_0 = 750$ K. Other parameters are detailed in the text. The inset show measured recombination kinetics on a linear-log scale, showing how the amplitude falls to zero at very low laser intensities (Ref. 14).

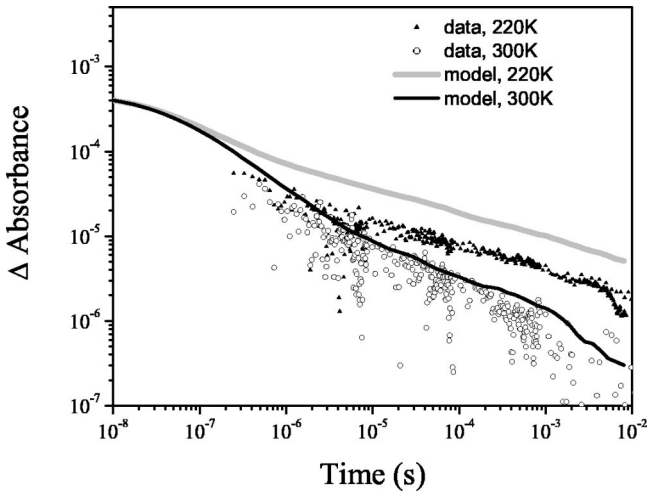

FIG. 4. Simulated kinetics at 300 and 220 K, in comparison with experimental data from Ref. 14 for laser intensities above the saturation threshold. Parameters are the same as in Fig. 3.

tinuously decreasing exponent while the exponent of the experimental data shows no further change below 200 K.

One explanation for the deviation from thermal activation is that at lower temperatures a second pathway, such as direct tunneling, becomes available to the polarons. We tested this by simulating the temperature dependent recombination in the tunneling model with different values of a_0 (data not shown). The model predicts temperature independent kinetics below 200 K only for values of a_0 greater than about $5a$. This value is unphysically large, and does not reproduce the data above 200 K correctly. One possibility may be that the localization radius increases at low temperature. At present we cannot explain the difference in amplitude between the measured and simulated 220-K data.

Figure 5 shows measured and modeled kinetics with and without background illumination at temperatures of 220 and 300 K. The modeled curves represent different background generation rates. In Fig. 5(b) both modeled curve are reduced in amplitude in order to show the effect of background light more clearly. All other parameters are as for Figs. 3 and 4.

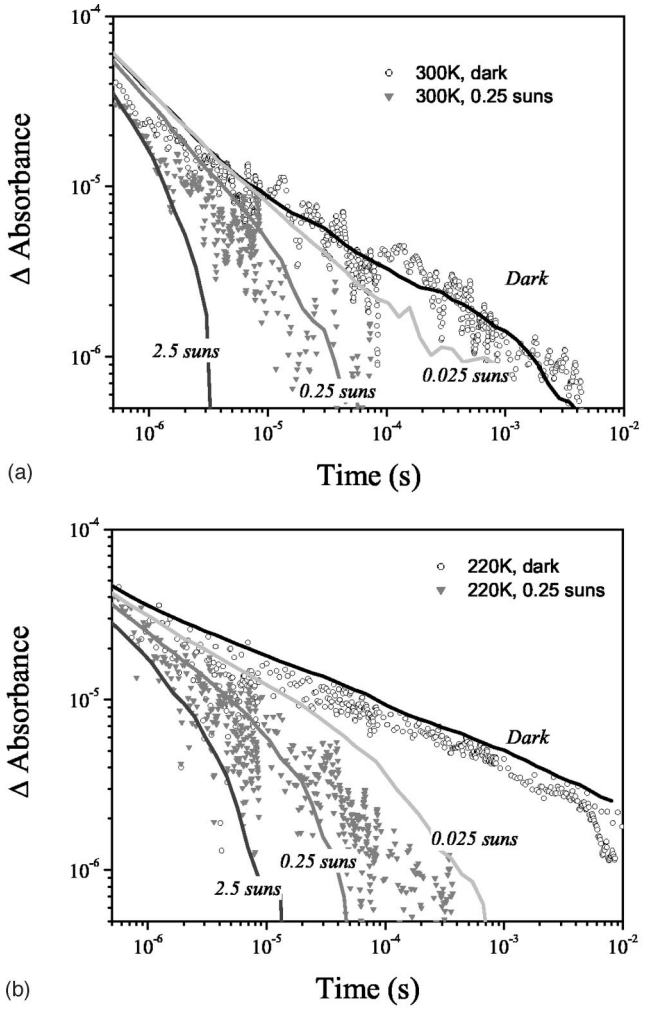

FIG. 5. Simulated kinetics under different levels of background illumination, in comparison with experimental data in the dark (open circles) and under background illumination equivalent to 0.25 suns at AM 1.5 (filled triangles) from Ref. 14. Laser pulse intensities are around 6–8 μJ per pulse. The 220-K model has been scaled to fit the experimental data in the dark, in order to show the effect of background light more clearly. Other parameters are as for Figs. 3 and 4.

From the measured absorption coefficient of MDMO-PPV we calculate that under one sun AM1.5 illumination the background generation rate should be 2×10^{21} cm^{-3} s^{-1}, which corresponds to one pair in the simulation volume every 20 μs. The experimental illumination is equivalent, in terms of photogeneration rate in MDMO-PPV, to about 0.25 AM1.5 suns. As Fig. 5 shows, simulations with this background generation rate are in good agreement with the data. The results may be explained physically as follows: under constant illumination, a steady state carrier density is established. These carriers fill the deepest traps. On exposure to the laser pulse, additional carriers are generated which occupy shallower states. Recombination then exceeds generation until the steady state is re-established. Recombination during this period removes only carriers occupying states above the steady state level and is therefore faster than it would be in the dark. Recombination events involving states below the steady state occupation level will be balanced by generation and will not be observed. Apart from the discrepancy in magnitude between data and model at 220 K, which was noted above, the model reproduces the effect of background light at both temperatures. Note that in both data and model the effect of temperature on kinetics is smaller under background illumination.

IV. DISCUSSION

The picture emerging from the previous section and the relevant experimental data, is as follows: (i) recombination in MDMO-PPV/PCBM blends is due to diffusional encounters between positive polarons and electrons on PCBM molecules; (ii) polaron motion is thermally activated, at least for temperatures above 200 K; and (iii) at low carrier concentrations, polarons are localized in a tail of trap states, but at higher concentrations the trap states become full and polarons occupy energy levels closer to the HOMO where transport is easier; (iv) the trap distribution may be modeled as an exponential.

The importance of trap states has been identified by previous studies on similar systems. Schultz *et al.* use time resolved electron spin resonance to study recombination kinetics in the same materials system at temperatures below 40 K.[15] They observe persistent charge carriers which decay following a power law in time, which they attribute to localization of positive polarons in sparse traps from which they escape by tunneling. Lee and co-workers observe power-law photocurrent transients in MEH-PPV/C60 blends which they attribute to trapping of charge carriers in localized states.[25] More recent time-of-flight mobility measurements in polyfluorene/PCBM systems indicate dispersive behavior at long times, again consistent with charge trapping in a tail of states.[26]

Schultz *et al.*, found temperature independent recombination kinetics at temperatures below 40 K, and modeled their data by considering direct tunneling from polaron to a PCBM anion using an excluded volume model due to Shklovskii *et al.*[27] This model is essentially identical to our tunneling model in the limit where $\nu_{pn}\gg\nu_{pp}$. Schultz *et al.* found a localization radius of around 1 nm and attempt to jump frequency of $\sim10^4$ s from modeling their data. In as far as can be tested, the model presented here is compatible with their results. Within the thermally assisted tunneling model, a localization radius of 1 nm leads to thermally activated behavior at temperatures above 200 K, indistinguishable from multiple trapping. It also leads to temperature independent behavior below 40 K. The rather low attempt to jump frequency reported by Schultz *et al.* is for a system where only polaron-anion events are allowed. If polaron hopping within the polymer phase were admitted, the data may be fit with a more realistic attempt to jump frequency.

The assignment of distinct fast and slow phases are supported by recent measurements of time resolved microwave conductivity on MDMO-PPV/PCBM blends by Savenije *et al.*[28] Those measurements show very similar dependence of charge carrier density on microwave intensity, with a fast ($<$100 ns) intensity dependent phase and a slow phase which

saturates with light intensities. This behavior is completely compatible with the bimodal density of states in our model. The concept of a bimodal density of states has also been invoked recently by Westerling *et al.* to explain different phases in optically observed recombination kinetics in regiorandom poly(3-hexylthiophene).[29]

Next we comment on the neglect of Coulomb interactions. The low dielectric constants of organic materials suggest that Coulomb interaction energies could be significant and might be expected to dominate charge recombination. However, Coulomb forces alone cannot explain the appearance or the saturation of the slow phase with light intensity. If Coulomb interactions were included in the model, these would affect the activation energy for either detrapping or thermally assisted tunneling by an amount $U_c = e^2/4\pi\varepsilon\varepsilon_0 r$, where e is the electronic charge, ε the dielectric constant, and r the charge pair separation. U_c varies from around 0.4 eV for charges separated by one lattice unit, to less than 0.02 eV for charge pairs at the mean separation for a light intensity of 1 μJ/pulse. The observable kinetics correspond to release from traps with activation energy over 0.25 eV. Therefore, for charge pair separations of over about 2 nm, the Coulomb interaction is negligible compared to the activation energy, and would not influence the results of simulation. For closer separations, Coulomb forces may enhance recombination but this can be represented within the model as a larger cross section for charge pair recombination, leading only to a lower attempt-to-jump frequency in the model. It is likely that Coulomb interactions influence the kinetics in the fast phase, where activation energies are smaller. However, the fast phase data are close to the resolution of the experiment and finding an accurate description is beyond the scope of this paper. We do not expect Coulomb interactions to change the temperature dependence of the kinetics, since for any given distribution of charges U_c, like the activation energies, is temperature independent. To a first approximation, U_c can be considered as a spatially dependent but temperature-independent modulation to the activation energy.

Finally we comment on our assumption that electron hopping does not influence kinetics. This follows from the surprising experimental observation that recombination kinetics are insensitive to PCBM concentrations up to ratios of 1:4 by weight. One explanation is that, in spite of the trapping of positive polarons, electrons are less mobile than holes in such blends. This is consistent with measurements of Refs. 26, 28, and 30, who found that electron transport improves with PCBM concentration, and dominates only at concentrations of over 85% by weight.[28] An alternative explanation is that electrons move more easily between fullerenes than between fullerenes and positive polarons, so that recombination is still limited by the transport of polarons towards fullerene domains in the blend. We have tested this idea by carrying out simulations with different concentrations of fullerene molecules. We consider the limit where electrons are fully delocalized between fullerenes so that the probability of recombination when a polaron meets a fullerene site is proportional to the ratio of fullerene anions to the total fullerene density. We find that at any given anion concentration, the polaron decay kinetics are virtually independent of fullerene concentration for fullerene concentrations from 0.01% to around 50% by volume, in agreement with the experimental data. However, we must stress that the model does not incorporate any interfacial effects, and the possibility that electron transport is influenced by the spatial segregation of fullerenes towards the surface of the film cannot be ruled out.

V. PHOTOCURRENT COLLECTION IN A SOLAR CELL

The previous sections supply a model for charge recombination in MDMO-PPV/PCBM blends at open circuit. Under solar illumination, multiple trapping of charge carriers dominates. This leads to long ($\sim$10 μs) carrier lifetimes at open circuit, favoring survival, but also prolongs the transit time for charge collection, and the net effect on photocurrent collection remains unknown. In this section we incorporate our model of polaron recombination and transport into a simple, one-dimensional device simulation order to establish whether the observed bimolecular recombination is relevant to solar cells under operating conditions. We focus on calculation of the short circuit current J_{sc} and consider how the presence of localized states affects the light intensity and temperature dependence of J_{sc}.

In the device simulation we solve a set of coupled one-dimensional transport equations for the steady state. We impose the usual charge continuity equations

$$\frac{1}{e}\frac{dJ_n}{dx} + G - R = 0, \tag{9a}$$

$$-\frac{1}{e}\frac{dJ_p}{dx} + G - R = 0, \tag{9b}$$

where J_n and J_p represent the electron and hole polaron current densities, G the bimolecular volume photogeneration rate, (which includes charge separation efficiency) and R the bimolecular recombination term. For electron transport, in the absence of any detailed information on the transport mechanism, we use a drift-diffusion expression

$$J_n = e\mu_n\left(nF + \frac{kT}{e}\frac{dn}{dx}\right), \tag{10a}$$

where μ_n is the electron mobility and the Einstein relation between diffusion and mobility is assumed. In the case of hole polaron transport we assume, in accordance with the multiple trapping model of polaron transport, that only *free* polarons (those lying above the mobility edge) can contribute to transport. Hence

$$J_p = e\mu_p(p)\left(pF - \frac{kT}{e}\frac{dp}{dx}\right) = e\mu_{\text{free}}\left(p_{\text{free}}F - \frac{kT}{e}\frac{dp_{\text{free}}}{dx}\right), \tag{10b}$$

where μ_{free} is the mobility of free polarons.

The same transport model implies that only free polarons can recombine. Hence

$$R = Bp_{\text{free}}n. \tag{11}$$

p_{free} is related to the total polaron density p via a relation of form (8). For a bimodal density of states, β is not necessarily equal to $1/\alpha$.

Finally, Poisson's equation is applied to take care of the electric field:

$$\frac{dF}{dx} = \frac{e}{\varepsilon}(p-n) \tag{12a}$$

and

$$\frac{d\phi}{dx} = -F. \tag{12b}$$

We use the model to simulate the short circuit photocurrent in a 100 nm thick polymer-fullerene blend sandwiched between poly(ethylene dioxythiophene) doped with polystyrene sulphonic acid (PEDOT) and Al contacts under AM1.5 illumination. The PEDOT interface is at $x=0$ and the Al interface at $x=d$. At short circuit, the current should be driven primarily by electric field in this system. We assume the boundary conditions that the potential drop through the sample is due to the difference in contact work functions, $\phi(d)-\phi(0)=\Delta\phi_{\text{work}}$, and that the contacts are perfectly selective, i.e., $J_n(0)=J_p(d)=0$ and $n(d)=p(0)=0$.

To implement the model, we need values for B, β, μ_{free}, and μ_n. Appropriate values of B and β for our distribution of states and operating conditions are obtained by simulations of the steady state, by fitting the steady-state simulated carrier density to the form $G=B(Ap^{\beta})p$. For the standard case we use $B=2.4\times10^{-15}$ m^3 s^{-1} and $\beta=1/\alpha-1$, an empirical relationship which fits the steady state simulations well over relevant temperatures and light intensities. The deviation of β from $1/\alpha$ is probably due to the increased density of states at the HOMO level. Nevertheless, provided that $\beta>1$, the exact form of β does not affect the qualitative results. Alternative combinations are presented in Fig. 6(b).

For μ_{free} we consider values in the range 10^{-4}–10^{-2} cm^2 V^{-1} s^{-1} in accordance with Ref. 28. This range is consistent with typical values, of order 10^{-2} cm^2 V^{-1} s^{-1}, of the mobility prefactor used in the Gaussian disorder model of Bässler[18] representing the mobility at the center of the density of transport states. For μ_n we take 5×10^{-5} cm^2 V^{-1} s^{-1}, consistent with recent time-of-flight measurements of electron mobility in polymer-PCBM blends at high PCBM concentrations.[26] G is assumed uniform and is taken as the average volume photogeneration rate for an absorption coefficient of 9×10^6 m^{-1} and an incident photon flux of 3×10^{20} cm^{-2} s^{-1} at one sun, in order to produce a photogeneration rate equivalent to AM1.5.

In Fig. 6(a) we present simulated J_{sc} at as a function of light intensity for three different values of μ_{free}. It is clear that J_{sc} increases linearly with light intensity, up to 1 sun, provided that μ_{free} is high enough. For the parameters used here, linear behavior requires $\mu_{\text{free}}>10^{-3}$ cm^2 V^{-1} s^{-1}, consistent with Ref. 28. This near-linear dependence is observed in devices[31] and is a key condition for efficient photoconversion. In simple terms, it indicates that the recombination observed by transient absorption is sufficiently slow compared to charge transport for all of the photogenerated charges to be collected at short circuit.

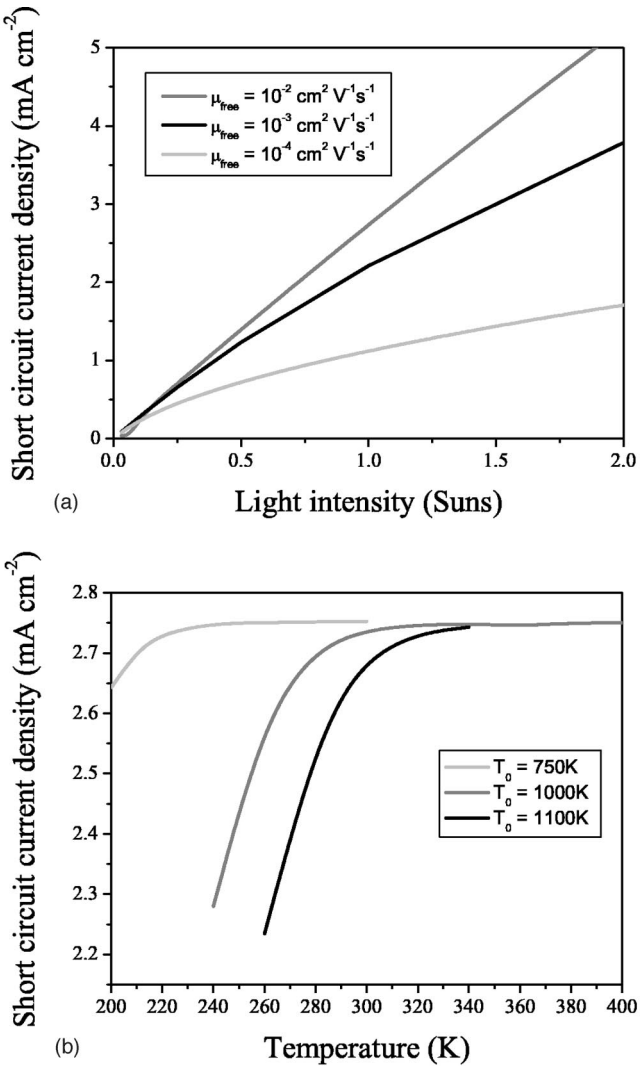

FIG. 6. (a) Calculated AM 1.5 short circuit photocurrent as a function of light intensity for different values of the free polaron mobility. Linear behavior is obtained if μ_{free} is high enough—over 10^{-3} cm^2 V^{-1} s^{-1} for the parameters deduced in this work. (b) Calculated AM 1.5 short circuit photocurrent as a function temperature, for different values of T_0 representing different shapes of the density of trap states. The decrease in J_{sc} as temperature falls is due to the distortion of electric field by the space charge of trapped polarons. A qualitatively similar behavior is reported in Ref. 31. Larger values of T_0 or β increase the trapping effect at any given temperature, although for parameters deduced in this work, space charge appears not to be limiting at room temperature.

In Fig. 6(b) we present simulated J_{sc} as a function of temperature, for different values of T_0. Here, for the parameters given above, we find that J_{sc} increases slightly as temperature is raised up to a saturation level. Exactly this type of behavior has been observed experimentally,[31] though at higher temperatures. It was previously attributed to thermally activated charge transport. However, our studies of recombination show that the recombination process is also thermally activated. In the limit where tunneling is negligible (as ex-

pected from small a_0) the effect of thermal activation on transport and recombination is identical: both are due to the increase in p_{free}. A change in temperature does not, therefore, change the branching ratio between transport towards the electrodes (collection) and recombination. The behavior in Fig. 6(b) is due to another effect. At lower temperatures, a higher fraction of polarons are trapped. These charges influence the distribution of electric field through Poisson's equation. At the lowest temperature in Fig. 6(a), the trapped charge density is sufficiently high that the electric field vanishes at the Al contact. This means that carriers generated close to that contact are less likely to be collected than if the field were constant, and more likely to recombine. Close to the opposite contact, the electric field is higher than average. However, this does not result in a similar reduction in recombination because collection under the average electric field is already very efficient. As the temperature is raised, less charge is trapped and the electric field becomes more even. The net effect of this is to reduce the recombination, and increase the photocurrent. Further increases in temperature cause no further change in electric field and the photocurrent saturates. Although the effect in Ref. 31 occurs at higher temperatures than predicted for the parameters deduced in this work (curve $T_0 = 750$ K), Fig. 6(b) shows that with different shapes of the density of states (equivalent to different expressions for β) the effect may be expected at room temperature.

VI. CONCLUSION

We have presented a model of charge transport and recombination in MDMO-PPV/PCBM blends, where recombination is limited by the diffusion of positive polarons through a landscape containing a small fraction (0.1%) of deep traps. The model is able to explain observed dependence of polaron recombination kinetics on laser intensity, temperature, and background illumination. At solar light intensities and room temperature, most polarons are trapped and therefore the release of polarons from the traps is the key process determining recombination times in photovoltaic devices. Simulations of photocurrent generation in a 100-nm-thick device indicate that, provided that the mobility of untrapped polarons is high enough ($>10^{-3}$ cm^2 V^{-1} s^{-1}) charge collection competes successfully with recombination under solar illumination at short circuit and leads to a linear dependence of photocurrent on light intensity, as observed. However, the space charge due to trapped charge reduces charge carrier collection at lower temperatures. This effect appears to explain the observed temperature dependence of short circuit photocurrent in plastic cells, which had previously been assigned to thermally activated hole mobility. Space charge effects may become more important in improved device designs with higher current densities.

ACKNOWLEDGMENTS

The author is grateful to James Durrant, Ivan Montanari, Ana Flavia Nogueira, Christoph Brabec, and Serdar Sariciftci for providing the experimental data prior to publication elsewhere and for many useful discussions; to Roberto Pacios and Donal Bradley for communicating results of mobility measurements; and to Dmitry Poplavskyy and James Durrant for a critical reading of the manuscript. Financial support from the EPSRC and the Greenpeace Environmental Trust is acknowledged.

[1] J. J. M. Halls *et al.*, Nature (London) **376**, 498 (1995).
[2] K. Yoshino *et al.*, IEEE Trans. Electron Devices **44**, 1315 (1997).
[3] G. Yu *et al.*, Science **270**, 1789 (1995).
[4] G. Yu and A. J. Heeger, J. Appl. Phys. **78**(7), 4510 (1995).
[5] B. O'Regan and M. Gratzel, Nature (London) **353**, 737 (1991).
[6] B. H. Erne, D. Vanmaekelbergh, and J. J. Kelly, J. Electrochem. Soc. **143**, 305 (1996).
[7] J. J. M. Halls *et al.*, Adv. Mater. **12**, 498 (2000).
[8] D. Vanmaekelbergh, A. Koster, and F. I. Marin, Adv. Mater. **9**, 575 (1997).
[9] C. J. Brabec, N. S. Sariciftci, and J. C. Hummelen, Adv. Functional Mater. **11**, 15 (2001).
[10] C. J. Brabec *et al.*, Appl. Phys. Lett. **80**, 1288 (2002).
[11] S. E. Shaheen *et al.*, Appl. Phys. Lett. **78**(6), 841 (2001).
[12] C. J. Brabec *et al.*, Chem. Phys. Lett. **340**, 232 (2001).
[13] I. Montanari *et al.*, Appl. Phys. Lett. **81**, 3001 (2002).
[14] A. F. Nogueira *et al.*, J. Phys. Chem. B **107**, 1567 (2003).
[15] N. A. Schultz *et al.*, Phys. Rev. B **64**, 245210 (2001).
[16] H. Scher and E. W. Montroll, Phys. Rev. B **12**, 2455 (1975).
[17] A. Jakobs and K. W. Kehr, Phys. Rev. B **48**, 8780 (1993).
[18] H. Bassler, Phys. Status Solidi B **175**, 15 (1993).
[19] S. V. Novikov *et al.*, Phys. Rev. Lett. **81**, 4472 (1998).
[20] J. Stephan, S. Schrader, and L. Brehmer, Synth. Met. **111**, 353 (2000).
[21] J. Nelson, Phys. Rev. B **59**, 15 374 (1999).
[22] J. Nelson *et al.*, Phys. Rev. B **63**, 205321 (2001).
[23] J. A. Anta, J. Nelson, and N. Quirke, Phys. Rev. B **65**, 125324 (2002).
[24] C. C. Moser *et al.*, Nature (London) **355**, 796 (1992).
[25] C. H. Lee *et al.*, Phys. Rev. B **48**, 15 425 (1993).
[26] R. Pacios *et al.*, Synth. Met. **137**, 1469 (2003).
[27] E. I. Levin, S. Marianer, and B. I. Shklovskii, Phys. Rev. B **45**, 5906 (1992).
[28] T. J. Savenije *et al.*, in *201st Meeting of the Electrochemical Society* (ECS, Philadelphia, 2002).
[29] M. Westerling *et al.*, Phys. Rev. B **66**, 165220 (2002).
[30] W. Geens *et al.*, Ph.D. Thesis, University of Antwerp, 2002.
[31] E. A. Katz *et al.*, J. Appl. Phys. **90**, 5343 (2001).